Modelling and optimization of hybrid renewable energy system using SBLA-MAT algorithm

Arun Kumar Udayakumar[1], P. Ashok[2], Mohan Das Raman[3], Krishnakumar Ramasamy[4], Mohammad Amir[5]

[1]Department of Electrical and Electronics Engineering, Karpagam Academy of Higher Education, Coimbatore, India
[2]Symbiosis Institute of Digital and Telecom Management (SIDTM), Symbiosis International (Deemed University), Pune, India
[3]Department of Electrical and Electronics Engineering, New Horizon College of Engineering, Bengaluru, India
[4]Department of Electrical and Electronics Engineering, Sri Ramakrishna Engineering College, Coimbatore, India
[5]Department of Energy Sciences and Engineering, Indian Institute of Technology (IIT), New Delhi, India

Article Info

ABSTRACT

In order to enhance the reliability and economic feasibility of power systems, this research presents a hybrid control method for the optimal design of hybrid renewable energy sources (RES), including fuel cells, solar photovoltaic (PV), and wind power. Optimization of the power system to enhance efficiency and reduce downtime is achieved using the side blotched lizard optimization with multi-objective artificial tree algorithm (SBL-MAT). The research intends to reduce costs in wind, PV, and FC scenarios and make it reliable for load delivery at a low cost and high level of dependability. While a mathematical model of SBL behavior demonstrates the need to discover and implement global optimizing approaches, the MAT algorithm resolves the supervised classification challenge. Possible benefits of the proposed technology include increased reliability and decreased maintenance costs for electrical systems. The proposed approach enables cost-effective and reliable load generation from PV, wind, and fuel cell systems, regardless of the volatility of the weather. Using MATLAB/Simulink, the assessment of parameters like recall, specificity, accuracy and precision is carried out and the results were 99.91%, 99.85%, 99.65%, and 99.325%, respectively. The parameters loss of load expectation (LOLE) and loss of energy expectation (LOEE) are calculated for analysis using both current and future technology.

Corresponding Author:

Arun Kumar Udayakumar
Department of Electrical and Electronics Engineering, Karpagam Academy of Higher Education
Coimbatore, Tamil Nadu 641021, India
Email: arun.udayakumarn@gmail.com

1. INTRODUCTION

Renewable energy sources (RES) have the ability to contribute significantly to addressing gaps in energy distribution. These sources provide a sustainable energy delivery method while simultaneously reducing local and global air pollution [1]. These phenomena may be ascribed to the notion that RES has a substantial potential to amplify imbalances in the energy distribution domain [2]. The use of distributed energy resources demonstrates significant engagement, mostly attributable to the cost-effective installation prerequisites associated with RES [3]. The inadequacy of energy in renewable energy source (RES) programs may be ascribed to the continual increase in energy demand, the finite nature of fossil fuels, and the worsening global conditions [4]. This methodology facilitates the production of electrical energy on the consumer side, especially in regions characterized by power networks with restricted capacity. To improve

the sustainability of outlying regions, the majority of the research has concentrated on standalone systems. Recent research on microgrids (MGs) evolved which are decentralized power systems that operate at lower voltage levels tackle energy difficulties at a local level effectively and facilitate the increase of capacity [5]. The system may function in either a grid-connected or island-based configuration, depending upon the existing circumstances [6]. Evaluating adaptive microgrids is essential, since future distribution networks will depend on novel smart grid concepts capable of functioning intelligently in diverse environmental conditions [7], [8]. Integrating photovoltaic (PV) producing units with wind production units in less densely populated regions offers a viable solution for meeting the energy demand [9], [10]. Furthermore, the inconsistencies in the sources do not align with the specified timeframe, and the expenses associated with addressing the reliability issues might be substantial [11], [12]. Hybrid systems may efficiently include non-essential characteristics of solar and wind production sources, resulting in improved system dependability and cost savings [13], [14]. The inconsistency and unpredictability of renewable energy sources (RES) provide a significant barrier to their swift integration into the power grid, hence limiting their potential for fast expansion in the future [15], [16]. In this particular scenario, we leverage the various impacts of renewable energy on the need for a spinning reserve. The most significant reserves have been optimized to provide between 0.3% and 0.8% of the total wind power generating capacity to continental power networks. Other reserves are expected to contribute between 6% and 10% [17]. In addition, it has been shown that using schematic generators might lead to a decrease in performance of up to 9% [18]. Integrating energy storage devices has improved the system's adaptability by effectively tackling these issues [19], [20]. Nonetheless, the economic integration of these systems mostly relies on capacity pricing, wind power potential, and investment costs [21], [22]. Demand response initiatives are a viable alternative, with projections indicating that their implementation in the Canary Islands may provide savings of about 30% [23], [24].

In recent years, there has been a notable surge in financial resources allocated towards research on RES. As a result, several renewable technologies, ideal for use in rural and outlying regions, have been available to developing nations. The most efficient way to deal with the growing demand for energy is to maximize the use of available resources. The suggested setup involves a proper connecting circuit linking solar PV sources to DC loads. Based on the DC source's power needs, DC interface circuits typically allow the DC/DC converter to provide power to the DC source. Renewable energy sources are becoming more popular and efficient, which will have positive effects on the economy and help reduce energy use. The mitigation of global warming via the reduction of pollution caused by the use of fossil fuels is expected to positively impact both the condition of nature and the overall health of the planet. Compared to other energy sources, large areas have substantial potential for utilizing renewable energy resources. The escalating prices of oil, constraints in oil supply, apprehensions about climate change, and global warming are anticipated to drive an upsurge in the demand for renewable energy. In this research, the analysis focusing reliability of a power system is carried out by a combination of renewable energy sources, including PV, wind turbines (WT), and fuel cells (FC). The SBL-MAT technique is a proposed hybrid approach that integrates the side-blotched lizard optimization [25] with the multi-objective artificial tree algorithm (SBL-MAT). The proposed work has the following contributions and advantages:
- Development of a simulation setup to derivate improved and optimized system efficiency.
- To compare and assess the parameters recall, specificity, accuracy, and precision of the proposed approach with existing approaches like genetic algorithm, particle swarm optimization, chemo-taxis algorithm (CA), Cuttlefish algorithm (CFA), May Fly-radial basis functional neural network (MA-RBFNN) technique and tunicate swarm algorithm (TSA) and GEO algorithm.
- Increasing the system reliability and reducing the production as well as operational costs.
- To analyze the system's loss of load expectation (LOLE) and loss of energy expectation (LOEE).

The subsequent portions of this work are outlined as follows: section 2 provides the detailed research gap analyzed. In section 3, the modelling of the SBL-MAT algorithm has been examined along with its comprehensive flowchart and analysis. The findings and examination of the simulation results for both the existing and new approaches are presented and deliberated in section 4. The article's conclusion and future scope are presented in section 5.

2. MOTIVATION AND RESEARCH GAP

Reliability and cost reduction in the power system have been briefly investigated using renewable energy sources. There was a fair amount of scope work in the new region. The literature review revealed that the particle swarm optimization method had a significant role in getting renewable energy sources to work more reliably and at a lower cost. The dependability of the power system and its cost have been enhanced and decreased by the use of additional approaches in an existing method. One way to make renewable energy sources less unstable is to use the time dependency approach. However, because of the attachment of

photovoltaic subsystems, the suggested approach has certain issues with delivering better dependability benefits. The filter selection method may determine the benefits of using a cluster of solar and wind turbine systems. The dependability has been measured in the presented approach based on the performance of every aspect of the system. The whole functioning of the system could be compromised if even a single component is damaged. In addition to improving the system's dependability, the particle swarm optimization (PSO) technique may lower the system's operating and maintenance costs. However, in some instances, the frequency variation problem is caused by renewable energy source concerns. The efficiency of the system is compromised by these issues with deviations. Consequently, the dispersed network did not get the dependable electricity that the design promised. To reduce these deviation concerns, additional money is needed. Studies depend heavily on wind and solar power, but there is a noticeable void in our understanding of other renewable energy sources. This is likely because there haven't been enough investigations into the models and technologies that may transform and combine various sources into integrated systems. As a result, the primary goals of a control strategy for a renewable energy system should be to keep an eye on the needed power, make the most efficient use of the available energy sources, and maintain a steady DC bus voltage in the MG-linked system. This problem can only be solved with an integrated MG system. These drawbacks and problems prompted this research because there are so few studies in the literature that provide solutions to this problem.

3.   MODELLING AND FORMULATION OF PROPOSED SYSYEM

This section provides a in depth analysis about the modelling and formulation of various components used in the proposed system along with the characteristics.

3.1. Modelling of solar PV

The solar cell, which is responsible for transforming solar energy into usable electricity, is the most crucial part of a PV system. When a PV cell is exposed to sunlight, a voltage or electric current is generated in the cell. A solar cell is made up of a light-absorbing material, like silicon. Electrons are jarred loose, allowing current to flow freely and creating a voltage difference. Solar photovoltaic systems can be installed on the ground, on a roof, on a wall, or even on water. A solar panel converts light energy into usable electricity by allowing photons to dislodge electrons from atoms. The semiconductor material formed the pn junction of the solar cell. An electron-hole pair is generated from the energy of photons when sunlight reaches a solar cell. The electrons and holes in the pair scatter, with the electrons moving into the n-region and the holes into the p-region, due to the electric field that is generated at the junction. Therefore, the voltage that a PV system produces is its output. Figure 1 displays the PV module schematic. Integral photocurrent (IPH) flows via the load that is linked to the cell's output terminals. An ideal photovoltaic cell's comparable circuit would include a diode and a current source linked in series. The terminals on the circuit's output are linked to the load. The (1) for the voltage-current relationship in a solar cell is here.

$$I_{pv} = I_{PH} - I_{DR}\left(e^{\frac{qV_{pv}}{Kt}} - 1\right)$$ (1)

The quantity of available sunlight at a given location determines how much electricity a PV cell can generate. The (2) is used to express the hourly output of the PV sequence.

$$P_{PV}^t = f_{PV} y_{PV}\left(\frac{I_t}{I_s}\right)$$ (2)

The (3) is used to get the PV panel output power from the backup information.

$$p_{pv} = \frac{S}{1000} p_{pv,rated} \times \eta_{pv}.Con_V$$ (3)

3.2. Modelling of WECS

The fundamental operating mechanism of wind turbines involves the conversion of kinetic energy present in the wind into rotational kinetic energy inside the turbine. Subsequently, this rotational kinetic energy may be harnessed to generate electrical energy, which can then be transmitted via the electrical grid. The components of a wind turbine include rotor blades, a yaw mechanism, an electronic controller, a hub, a gearbox, a high-speed shaft with a mechanical brake, a low-speed shaft, a hydraulic system, a tower, an anemometer, a wind vane, and a cooling unit. Wind turbines have the capability to revolve around either a vertical or a horizontal axis. The horizontal axis wind turbine is characterized by the placement of its rotors upwind of the supporting tower. The wind turbines used in wind farms for the purpose of industrial electricity generation typically consist of three blades. The reduction in ripple torque results in enhanced dependability.

The use of gearless turbines for the purpose of eliminating gear speed has resulted in increased costs associated with permanent magnet direct drive generators. The monitoring of the gearbox and equipment in wind turbines is often conducted by using many accelerometers and strain gauges affixed to the nacelle, owing to challenges associated with data transmission. The achievement of changing the reference signal of the pulse width modulation (PWM) in each leg is facilitated by the reference signal in the gating circuit for the insulated gate bipolar transistor (IGBTs). The gating signals are generated by the process of comparing a sinusoidal reference voltage with a triangle waveform. Figure 2 illustrates the power circuit control and block diagram of a wind turbine. In the fundamental functioning of the circuit, the comparator will provide an output of one when the sinusoidal voltage exceeds the triangle waveform, while the output will be zero in all other cases. The equation provided in the WT expresses the relationship between the turbine's output power and torque with respect to its rotating speed.

$$P_{WT} = 0.5 a_{density} B_c(\mu, \delta) \left(\frac{T_r \cdot \omega_{os}}{\lambda_{os}}\right)^3 \tag{4}$$

$$T_\tau = 0.5 a_{density} B_c(\mu, \delta) \left(\frac{T_r}{\lambda_{os}}\right)^3 \omega_{os} \tag{5}$$

The equation of the wind turbine and speed are expressed as (6).

$$P_{WT} = \begin{cases} \frac{V^2 - V_{cinws}^2}{V_{rated}^2 - V_{cinws}^2} \cdot P_{rated}; V_{cin_{ws}} \leq V \leq V_{rated} \\ P_{rated}; V_{rated} \leq V \leq V_{cows} \\ 0; V \leq V_{cinws} \, and \, V \geq V_{cows} \end{cases} \tag{6}$$

$$\omega_{output} = \frac{\lambda_{output}}{r_s} \cdot V_{ws} \tag{7}$$

The Cp-TSR characteristic is used to denote the WT, as seen in Figure 3. In order to determine the power output of a wind energy system (WES), the wind speed recorded at the height of the anemometer is first modified to align with the appropriate center height via the use of the power frame profile.

$$TSR = \frac{S_M R}{V} \tag{8}$$

The assessment of power output involves the determination of the power curve of the wind turbine. The relationship between wind speed and photovoltaic (PV) array may be described by (9).

$$P_{wt}^t = \begin{cases} 0 & 0 \leq v \leq v_{cutin} \, and \quad v \geq v_{cutout} \\ a \times v^3 + b \times P_{rated} & v_{cutin} \leq v \leq v_{rated} \\ P_{rated} & v_{rated} \leq v \leq v_{cutout} \end{cases} \tag{9}$$

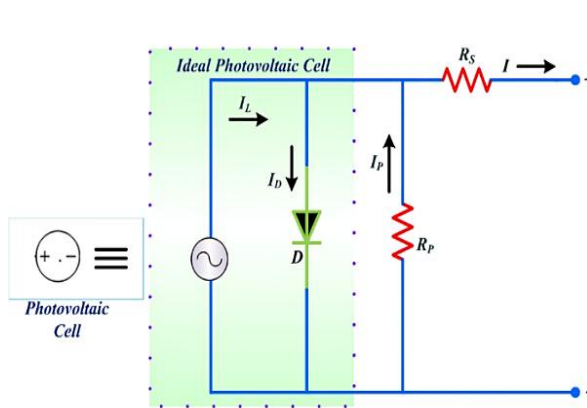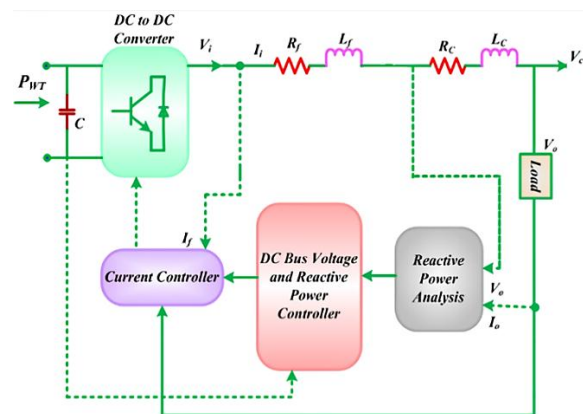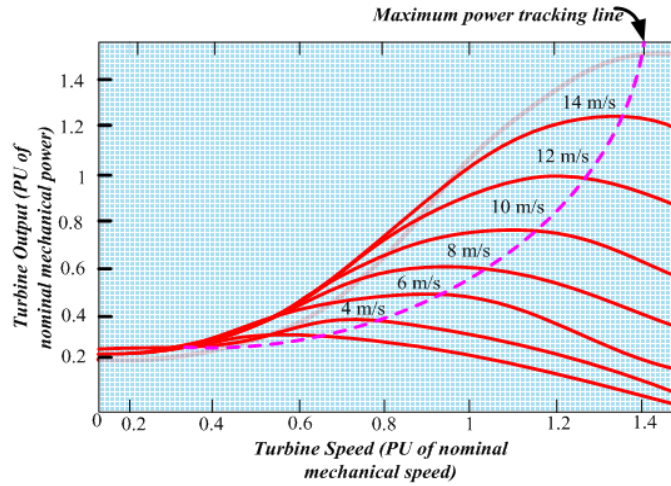Figure 1. Modelling of PV cell   Figure 2. Modelling and control of WECS

Figure 3. C_P – TSR characteristic of the wind generation system

3.3. Modelling of fuel cell

Fuel cells (FC's) are electrochemical devices that efficiently transform chemical energy into electrical energy via direct conversion. The FC has certain performance characteristics when subjected to non-uniform distribution, and it is economically viable when used on a large industrial scale. The FC has superior performance in terms of high stability production and demonstrates a more robust and dynamic reaction. The functional relationship between the input of the fuel cell (FC) and its output power is used to describe the power output of the FC. The evaluation of the performance of FC is outlined as (10).

$$p_{\text{fuelc}} = Fuel.\text{c} \times \eta_{\text{fuelc}} \tag{10}$$

3.4. Operating strategy and methodology of proposed system

The estimation of power delivered to the DC bus from renewable sources may be achieved by describing the outputs of photovoltaic (PV) and wind turbine (WT) systems.

$$p_{ren}\left(\eta_{wt}^{Fail}.\eta_{pv}^{Fail}\right) = \left(n_{wt} - \eta_{wt}^{Fail}\right) \times p_{wt} + \left(n_{pv} - \eta_{pv}^{Fail}\right) \times p_{pv} \tag{11}$$

Here, we provide information about the installed capacity of photovoltaic (PV) and wind turbine (WT) systems, denoted as $n_{wt} and n_{pv}$, as well as the corresponding failure rate of PV and WT systems, denoted as $\eta_{wt}^{Fail}, \eta_{pv}^{Fail}$. The dependability of the system is influenced by the presence or absence of the system. Furthermore, the energy derived from renewable sources is dissipated via two distinct mechanisms. Firstly, a portion of the energy is allocated to the DC/AC inverter in order to fulfill the load requirements. Secondly, any surplus energy is used for the purpose of hydrogen generation, where it undergoes conversion through the process of electrolysis. The algorithm of the operating system consists of a set of functions, which are enumerated below:

-   If, $p_{Re\,n}(t) = \frac{p_{load}(t)}{\eta_{inv}}$, The aggregate power produced by the inverter via the use of sustainable energy sources is then integrated with the electrical loads.
-   If, $p_{ren}(t) > \frac{p_{load}(t)}{\eta_{inv}}$, The power that is introduced subsequently produces the designated power of the electrolyte and any surplus power is subsequently transformed into electrolyte.
-   If, $p_{Re\,n}(t) < \frac{P_{Load}(t)}{\eta_{inv}}$ The power deficit is then allocated by the fuel cell. In the event that the distributed power above the rated power of the fuel cell, the distribution is not extended via the use of hydrogen. This concept may be further applied to the phenomenon of load loss.

3.5. System reliability determination model

In this part, we will discuss the impact of PV systems, WT, and DC/AC converters on the overall system. The probability of each state is estimated based on the dual distribution function. The (12) represents the chance of transitioning between states.

$$F_{ren}\left(\eta_{wt}^{Fail}.\eta_{pv}^{Fail}\right) = \left[\binom{n_{wt}}{\eta_{wt}^{Fail}} \times g_{wt}^{n_{|wt} - \eta_{wt}^{Fail}} \times (1 - g_{wt})^{\eta_{wt}^{Fail}}\right]$$

$$\times \left[\binom{n_{pv}}{\eta_{pv}^{Fail}} \times g_{pv}^{n_{pv} - \eta_{pv}^{Fail}} \times (1 - g_{pv})^{\eta_{pv}^{Fail}} \right] \tag{12}$$

The evaluation of the steady state dependability of the DC/AC converter is presented as (13).

$$g_{inv} = \frac{MTTF_{inv}}{MTTF_{|inv} + MTTR_{inv}} \tag{13}$$

In this context, MTTF is referred to as mean time to failure, whereas MTTR is referred to as mean time to repair.

4. SIDE-BLOTCHED LIZARD OPTIMIZATION ALGORITHM (SBL ALGORITHM)

Figure 4 shows the proposed building block of reliability and cost optimization of the power system with the SBL-MAT algorithm. Electricity consumers should ensure the power grid's stability at the lowest possible cost. Energy may be mostly harnessed from solar and wind sources. Renewable energy sources are unable to provide electricity and ensure reliable power transmission to various companies due to worries around system outages and environmental challenges. The cost of the electrical infrastructure is a critical concern. The elevated expense of the power system results in reduced consumption, thus leading to unmet energy requirements. Previous sections used various strategies to reduce power system costs and enhance reliability. Nevertheless, the approach would not get us to the location necessary to complete this task. This section presents two techniques that might enhance power system reliability and reduce associated costs. The methods under consideration are the multi-objective artificial tree (MAT) algorithm and the side-blotched lizard optimization (SBL) algorithm. The SBL-MAT algorithm is designed to optimize multiple objectives at once, which is crucial for managing the trade-offs between economic, environmental, and operational goals in renewable energy systems.

The side-blotched lizard methodology (SBL) is an optimization method that emphasizes subpopulations. The objective is to ascertain the total and partial populations of lizards, while accounting for the gradual changes in the distribution of each morph over time. The study of lizards entails the analysis of three unique morphs linked to certain mating behaviors. This approach involves the analysis of three unique polymorphisms or subpopulations: blue, orange, and yellow lizards. It is essential to recognize that these subpopulations arise only after the formation of the original population. Three principles—protective, expanding, and sly—are used to clarify the mating behavior of each morph. The collaborative effort of the morphs leads to the establishment of a polymorphic population capable of sustaining balance among the subpopulations of each morph without diminishing the least dominant morph. The examination of these reptiles is vital for evaluating insular colonization and extinction, genetic bottlenecks, ecology, and other essential evolutionary issues. The potential effect of this mechanism is in its capacity to use the array of solutions for tackling multi-objective challenges. Furthermore, it may be used in practical situations to assess its effectiveness from many perspectives.

4.1. Steps followed in the SBL algorithm

- Step 1: Initialization: Use (14) and (15) to set the starting lizard population.

$$X = 1, 2, \ldots t_{CRE} \tag{14}$$

$$Y = 1, 2, \ldots . D \tag{15}$$

Where, t_{CRE} is the total number of creatures or populations.
- Step 2: Random generation: The (16) should be used to produce the monsters at random after startup.

$$S = \begin{pmatrix} S_{11} & S_{12} \ldots . \\ S_{21} & S_{22} \ldots . \\ S_{31} & S_{32} \ldots \ldots \end{pmatrix} \tag{16}$$

- Step 3: Fitness function: Determine the healthiness of all search lizards. The evaluation of healthiness is based on the objective function. It is stated as (17).

$$p_{MAX} = \left(tcre * \frac{2}{p_{sub}} - p_{MIN} \right) \tag{17}$$

- Step 4: Sub-population creation: Use (18) to generate the sub-creatures for each iteration.

$$p_{ITER} = U + V^* Sin\left(S + \left(\frac{f}{p_{SUB}} * I\right)\right) \tag{18}$$

- Step 5: Comparison: In order to conduct a comparative analysis of lizard coloration, it is necessary to examine the coloration of various lizard species.
- Step 6: Termination: The procedure will go to step 3 if the lizard's color does not match the colors of the other lizards. Otherwise, the process will be canceled.
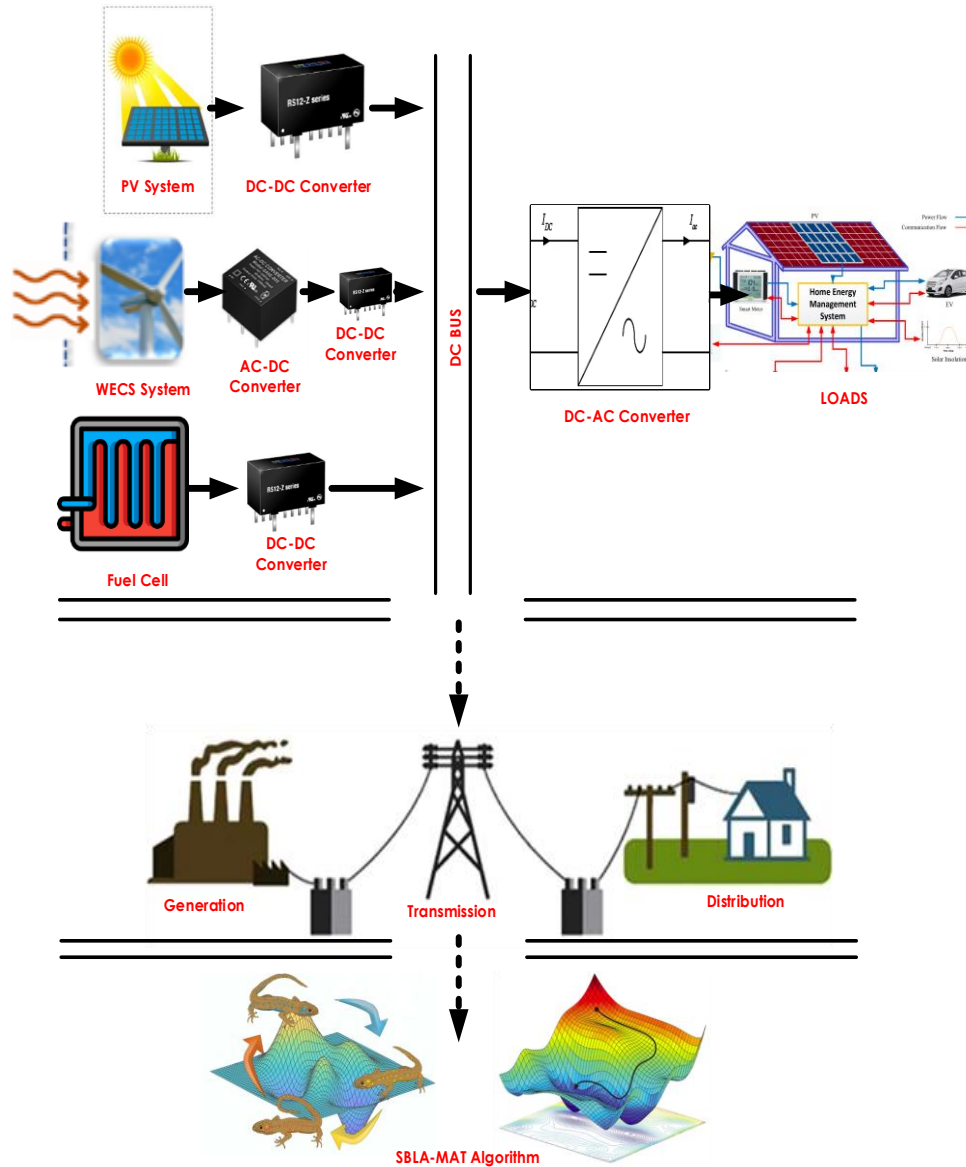

Figure 4. Proposed SBL-mat algorithm for reliability and cost optimization of the power system

4.2. Multi-objective artificial tree (MAT) optimization algorithm

Figure 5 shows the proposed SBL-MAT algorithm for the reliability and cost optimization of the power system. The MAT optimization method is used to examine the organic matter conversion process from leaves to various tree components, as well as the construction of branches. The design variables include the placements of branches. Moreover, the larger branches exert dominance over the smaller branches. The transmission function of biological matter occurs via the production of new branches. The updating of branches plays a crucial part in analyzing all the functions of MAT. In this context, the cross-over and self-evolution operator approaches have been used to modify and enhance the branches. When the branch is updated using the cross-over operator, there is no data exchange between the branches. When the branch is

updated using the self-evolution operator, it just considers its own data. Generating additional branches may be achieved by using (19)-(21).

$$S_l = S_I + RAND(0,1)x\left(S_{Leader} - S_J\right) x\ C_1 \qquad (19)$$

$$S_r = S_I + RAND(0,1)x\left(S_{Leader} - S_I\right) x\ C_2 \qquad (20)$$

$$S_{New} = RAND(0,1)xS_l + RAND(0,1)\ x\ S_r \qquad (21)$$
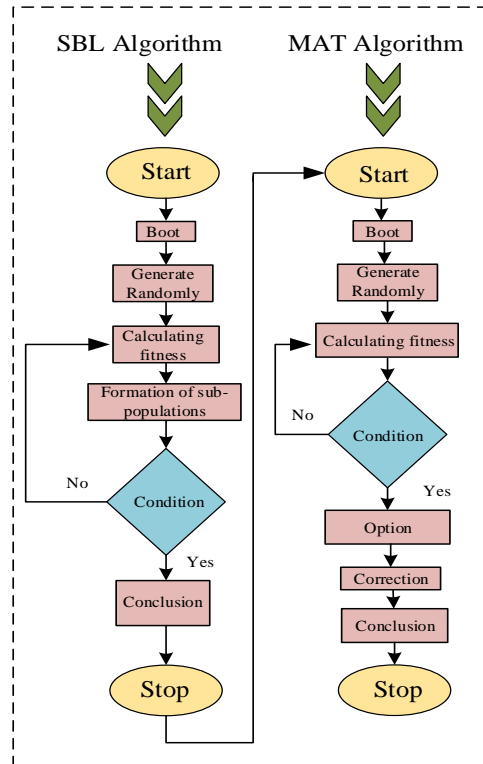
Figure 5. Flow chart of the MAT algorithm

4.2.1. Parameters of the MAT algorithm

Spread: Spread refers to how well the solutions are distributed across the Pareto front. In multi-objective optimization, the objective is not only to find optimal solutions but also to ensure that the solutions are spread out over the entire range of possible trade-offs between the conflicting objectives. A good spread indicates that the algorithm has successfully explored a wide variety of solutions across the Pareto front, leading to a diverse set of non-dominated solutions. The value of the spread is given using (22).

$$spread = \frac{\sum_{I=1}^{M} D(P_I,a) + \sum_{S \not\exists a} |D(S,a) - \bar{D}|}{\sum_{I=1}^{M} D(P_I,a) + |a|\bar{D}} \qquad (22)$$

Where PI = equally distributed points, M = No. of branches, and D = Distance.

Inverted generational distance (IGD): "IGD" refers to the metric used to measure the distance between a beginning point and an ending location. The assessment of the IGD's value may be conducted using (23).

$$igd(a,w) = \frac{\sum_{V \not\exists w} D(V,a)}{|w|} \qquad (23)$$

Hypervolume (hv): The hyper volume is a metric used to evaluate the quality of a set of solutions. It measures the volume of the objective space dominated by a Pareto front (a set of non-dominated solutions). The hyper volume indicator helps compare different Pareto fronts; a larger hypervolume generally indicates better solutions. The hv can be represented as (24).

$$hv = Vol(\cup_{S \nexists a} [F_1(S), q_1]x[F_2(S), q_2]x \ldots \ldots x[F_N(S), q_N] \tag{24}$$

Where N = Number of branches and q = reference value. The sequential procedure of the MAT algorithm is presented as follows:
- Step 1: Initialization: Initialize the number of branches as (25).

$$B=\{B_1, B_2, B_3 \ldots \ldots B_N\} \tag{25}$$

- Step 2: Random generation

$$B = \begin{pmatrix} B_{11} & B_{12} \ldots \ldots \\ B_{21} & B_{22} \ldots \ldots \\ B_{31} & B_{32} \ldots \ldots \end{pmatrix} \tag{26}$$

- Step 3: Fitness function: The fitness value for each branch point may be determined using (27).

$$B_{FIT} = RAND(0,1)xB_l + RAND(0,1)xB_r \tag{27}$$

- Step 4: Comparison: Evaluate the additional branches in light of the existing tree.
- Step 5: Selection: The thicker of the two branches will be chosen as the non-dominant.
- Step 6: Upgradation: With updated operators, we can keep the number of branches up to date.
- Step 7: Termination: If the desired optimal point is not reached, the procedure resumes at step 3; otherwise, it ends. Figure 5 is a flowchart illustrating the MAT and SBL optimization algorithms.

5. RESULTS AND DISCUSSIONS

This section presents an explanation of the simulation results and a discussion pertaining to power system reliability and cost minimization. The proposed technique, based on the SBL-MAT, is introduced to enhance power system reliability and reduce costs. The effectiveness of the proposed system is then compared to existing systems like genetic algorithm, particle swarm optimization, chemo-taxis algorithm (CA) [26], cuttlefish algorithm (CFA) [27], may fly-radial basis functional neural network (MA-RBFNN) technique [28] and tunicate swarm algorithm (TSA) [29] and GEO algorithm [30].

5.1. Simulation parameters and specifications

Simulation parameters, solar PV system specifications (for a single solar panel – output of 300 W) (77 panels are connected to get the output of 23 kW) are shown in Table 1. The simulation parameters for the wind energy conversion system (3×7.5 kW WECS systems) are shown in Table 2. The simulation specifications for the fuel cell system are shown in Table 3.

Table 1. Simulation parameters of solar PV system

Parameter	Values	Parameter	Values
Module temperature	28 °C	Capacitance of boost converter	0.611 µF
No of solar cells in series	72	Inductance of boost converter	0.763 mH
No of rows of solar cells in parallel	4	Switching frequency of PWM	100 KHz
Output voltage	12 V	Proportional gain of PI controller (K_P)	0.006
Output Power	300 W	Integral gain of PI controller (K_I)	7

Table 2. Simulation parameters of WECS

Sub-systems	Specification	
Wind turbine	Type	Horizontal three-bladed
	Rated power	7.5 kW
	Rated wind speed	9 m/s
	Rated turbine speed	1500 RPM
Electrical generator	Type	Squirrel cage induction machine
	Number of Phases	3
	Rated voltage	250 V
	Rated power output	7.5 kW
	Rated speed	1500 RPM
The VVVF drive	Type	Three-phase Graetz bridge
	Rated power	10 kW
Battery	Type	Lead Acid
	Capacity	1500 AH, 600 V

<p style="text-align:center">Table 3. Specifications of fuel cell</p>

Type of fuel cell	Electrolyte	Operating level (°C)	Size of stack	Efficiency
Polymer electrolyte membrane (PEM)	Perfluoro sulfonic acid	< 120	< 1-100 kW	> 80%

Power analysis of the suggested method is shown in Figure 6, with three systems—a PV system, a wind system, and a fuel cell—being examined in particular. Figure 6(a) shows that throughout the specified time period of 7100 hours, the power reaches its maximum value of 27 W. Figure 6(b) shows that at 8600 hours, the power value peaks at 24 W. Within 2500 hours, the power reaches its maximum value of 15 W, as shown in Figure 6(c).

(a)

(b)

(c)
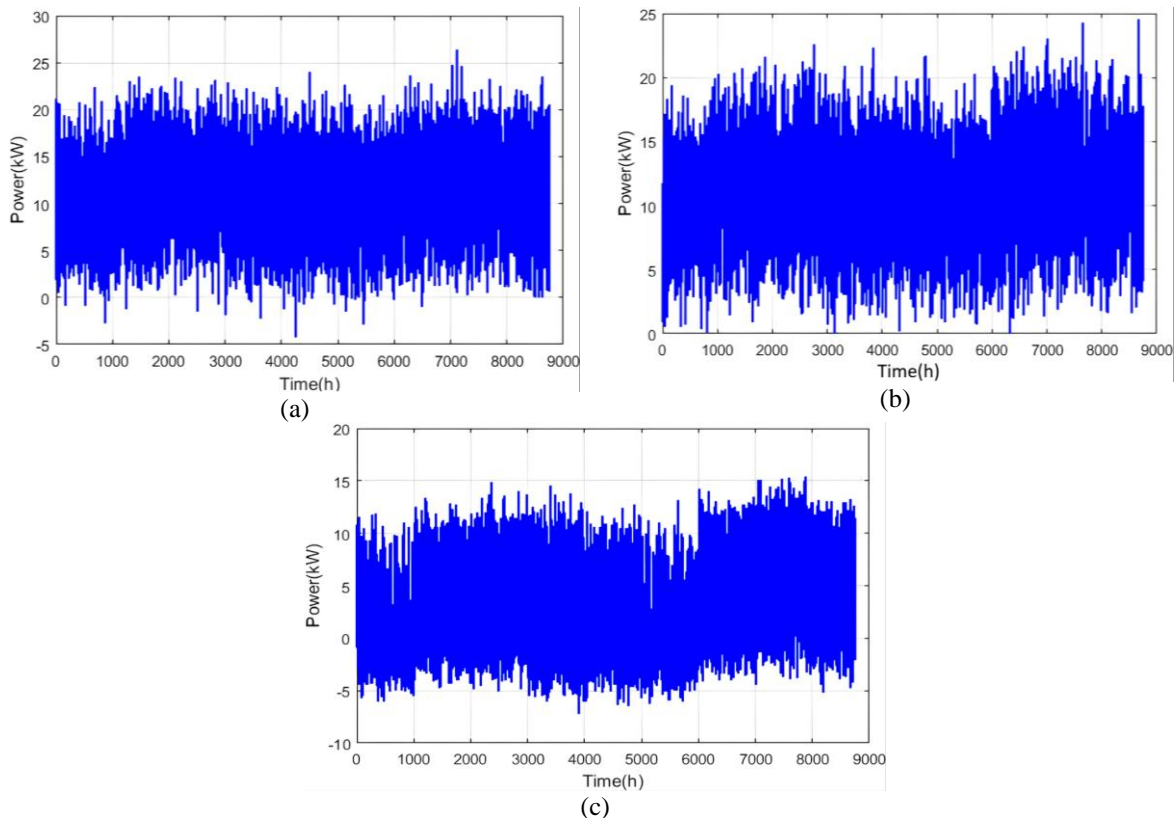
Figure 6. Power analysis of proposed method: (a) PV system, (b) wind system, and (c) fuel cell

Figure 7 shows the cost comparison of the suggested and existing methods. The cost of the offered method ranges from 0.5×10^7 to 1.9×10^7 \$. Figure 7(a) shows the comparison cost of the genetic algorithm and particle swarm optimization approaches. The cost range of the genetic algorithm is 2.7×10^7 \$ and the PSO algorithm is 2.2×10^7 \$. Figure 7(b) compares the costs of the suggested CA methods and those already in use. The current CA range costs 2.5×10^7 \$, and the recommended range is 1.9×10^7 \$. Figure 7(c) shows how the new and current CFA methods compare regarding cost. The current cost range for the CFA is 2.4×10^7 \$ and the suggested range is 1.9×10^7 \$. Figure 7(d) shows how the planned and current TSA methods compare regarding cost. The current range of TSA costs is 2.1×10^7 \$, and the suggested range is $1.9 x 10^7$ \$. Figure 7(e) shows a comparison of the costs of the suggested MA-RBFNN methods and those that are already in use. The current cost range for MA-RBFNN is 2.0×10^7 \$, and the suggested cost range is 1.9×10^7 \$. Figure 7(f) shows the comparison costs of the proposed and GEO-SN^{2}L approaches. The existing approach provides a cost range of 2.1×10^7 \$ and the proposed cost range is 1.9×10^7 \$.

Figure 8 shows how the proposed and current methods compare in terms of cost. The cost of the offered method ranges from 0.5×10^7 to 1.9×10^7 \$. At 0 h, the price can be anywhere from 0.5×10^7 to 1.9×10^7 \$. At 2000 h, the price of the system is 1.7×10^7 \$. The cost of the current method can range from 0.3×10^7 to 2.5×10^7 \$. The cost of the current method is higher than that of the proposed system. A comparison of the suggested technique to the current one is shown statistically in Table 1. The results of

conventional GA and PSO algorithms are 1.5874/1.4755, 1.4791/1.3763, and 0.5773/0.1491 for the mean, median, and standard deviation, respectively. The results from the CFA system are 1.0656, 0.9462, and 0.2465 for the mean, median, and standard deviation, respectively. The TSA system obtains mean values of 0.9641, median values of 0.9794, and standard deviation values of 0.1146. The MA-RBFNN system returns values of 0.9456, 0.9441, and 0.1068 for mean, median, and standard deviation, respectively. The GEO-SN2L system gets means of 0.9145, medians of 0.9052, and standard deviations of 0.0985. The suggested approach obtains means and variances of 0.9241, 0.9141, and 0.1012, respectively. In this case, the proposed technique outperforms the existing methods.

The suggested method's cost breakdown is shown in Figure 9, as Figure 9(a) LOEE with LOLE, Figure 9(b) LOEE with annual cost, and Figure 9(c) LOLE with annual cost. Figure 9(a) shows that when LOLE is 65 h/year, LOEE peaks at 230 MWh/year. Figure 9(b) shows that at an annual host of 3.15, LOEE peaks at 230. The LOEE value decreases until the yearly cost is \$3.18, then holds steady at the \$3.20 level afterward. Figure 10(a) shows that the loss of energy expectation (LOEE) registers as zero at specific points, precisely at LOLE values of 10, 30, 50, 70, and 90. Figures 10(b) and 10(c) demonstrate a consistent absence of LOEE across all possible yearly costs.
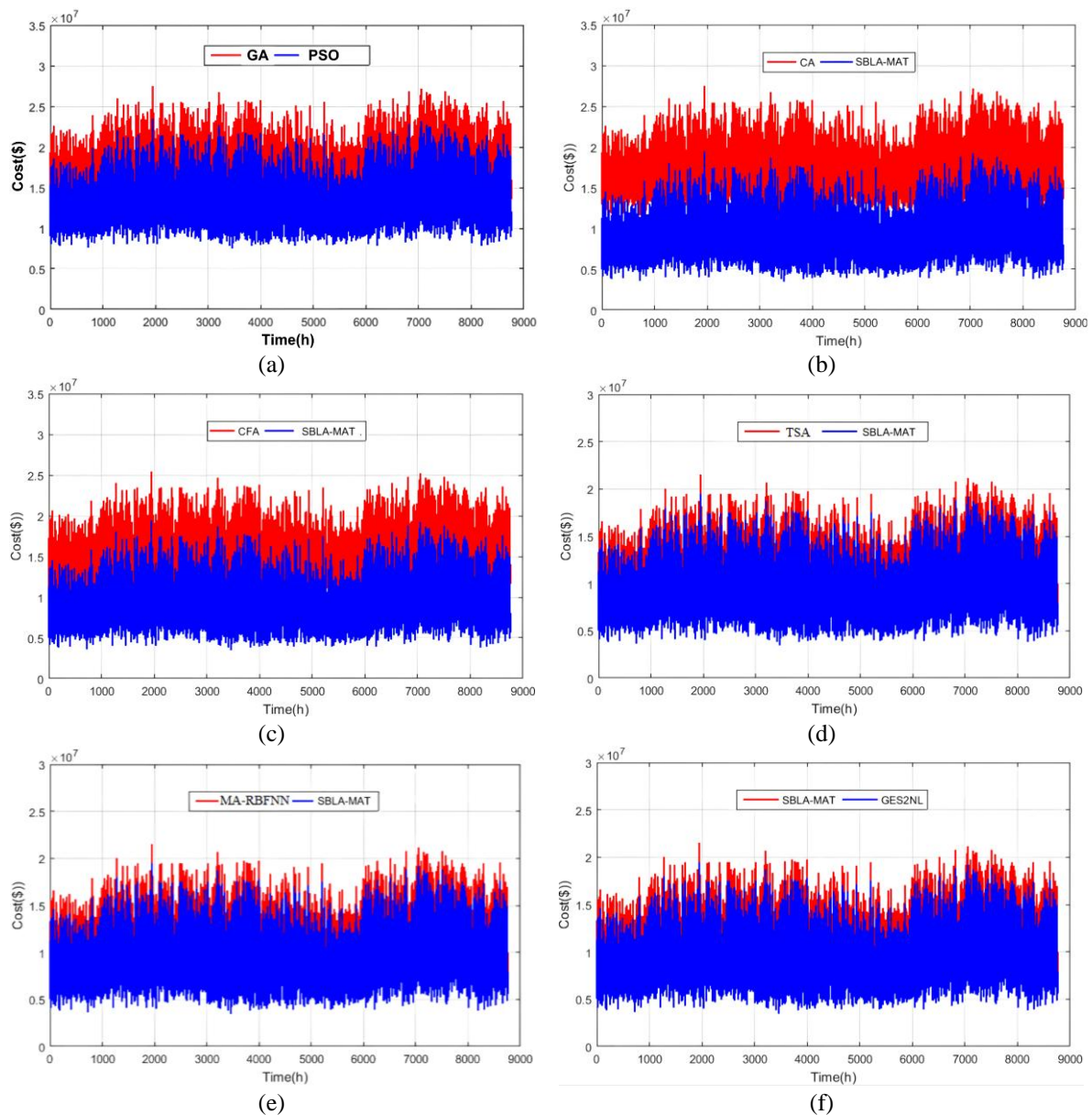
Figure 7. Cost comparison of (a) GA with PSO, (b) CA with proposed, (c) CFA with proposed, (d) TSA with proposed, (e) MA-RBFNN with proposed, and (f) GEO-SN^{2}L with proposed
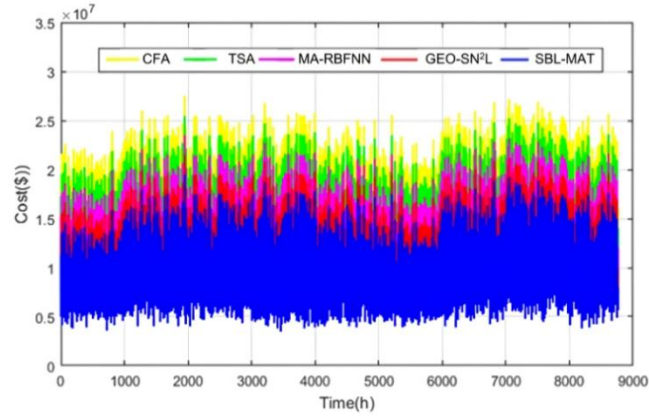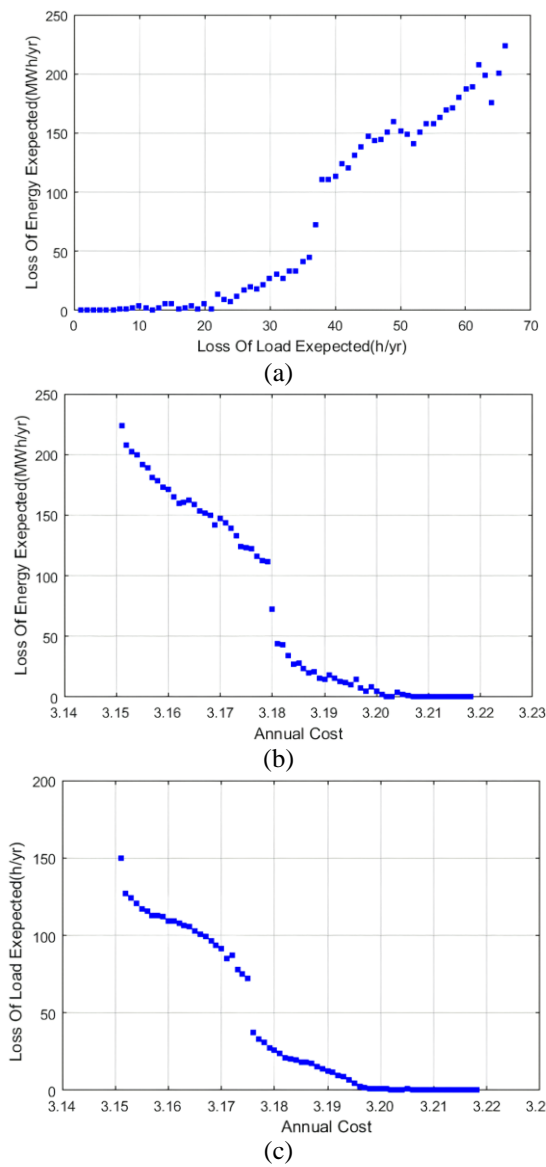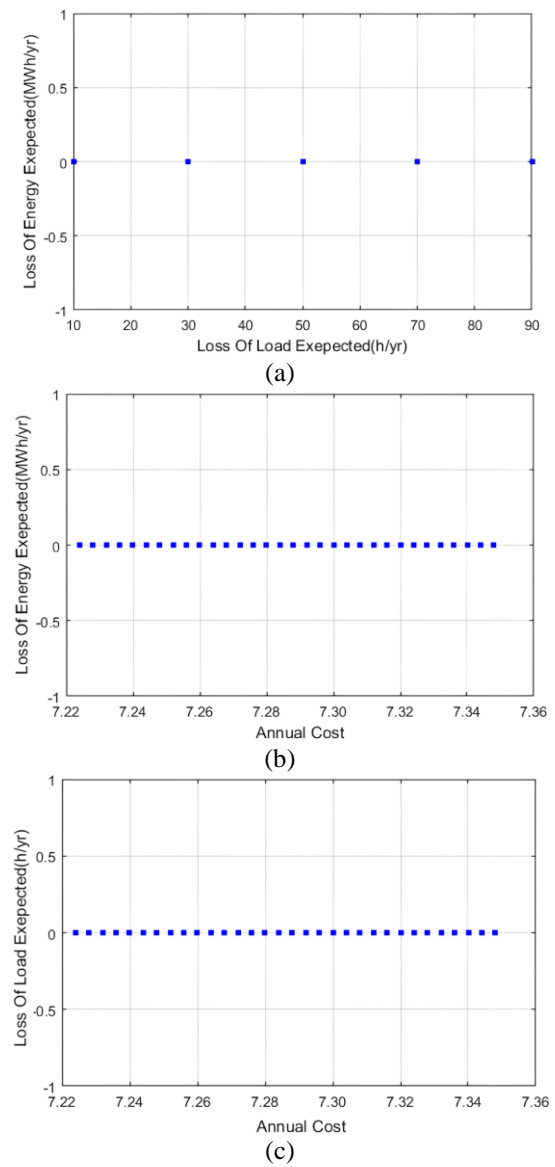
Figure 8. Cost comparison of existing and proposed approaches

Figure 9. Cost analysis of the proposed method:
(a) LOEE with LOLE, (b) LOEE with annual cost,
and (c) LOLE with annual cost

Figure 10. Cost analysis of the proposed method:
(a) LOEE with LOLE, (b) LOEE with annual cost,
and (c) LOLE with annual cost

Moving to Figure 11(a), it becomes evident that LOEE remains at zero until the LOLE reaches 30. Beyond this threshold, as the LOLE increases, the LOEE attains its maximum value of 350 at an LOLE of 300. Transitioning to Figure 11(b), the graph indicates that LOEE reaches its peak at a cost of 3.75 per year. Interestingly, it then sharply declines to zero as the yearly cost escalates to 3.82 per year. In Figure 11(c), the maximum LOLE is depicted as 200 at a cost of 3.74 per year. Subsequently, the yearly cost increases to 3.84, causing the LOLE to drop to zero. These observations suggest a complex interplay between LOLE, LOEE, and annual costs, emphasizing the importance of understanding these dynamics for the system or process under consideration.

A comparison of the suggested technique to the current one is shown statistically in Table 4. The results of conventional GA and PSO algorithms are 1.5874/1.4755, 1.4791/1.3763 and 0.5773/0.1491 for the mean, median, and standard deviation, respectively. The results from the CFA system are 1.0656, 0.9462, and 0.2465 for the mean, median, and standard deviation, respectively. The TSA system obtains mean values of 0.9641, median values of 0.9794, and standard deviation values of 0.1146. The MA-RBFNN system returns values of 0.9456, 0.9441, and 0.1068 for mean, median, and standard deviation, respectively. The GEO-SN^{2}L system gets means of 0.9145, medians of 0.9052, and standard deviations of 0.0985. The suggested approach obtains means and variances of 0.9241, 0.9141, and 0.1012, respectively. In this case, the proposed technique outperforms the existing methods.
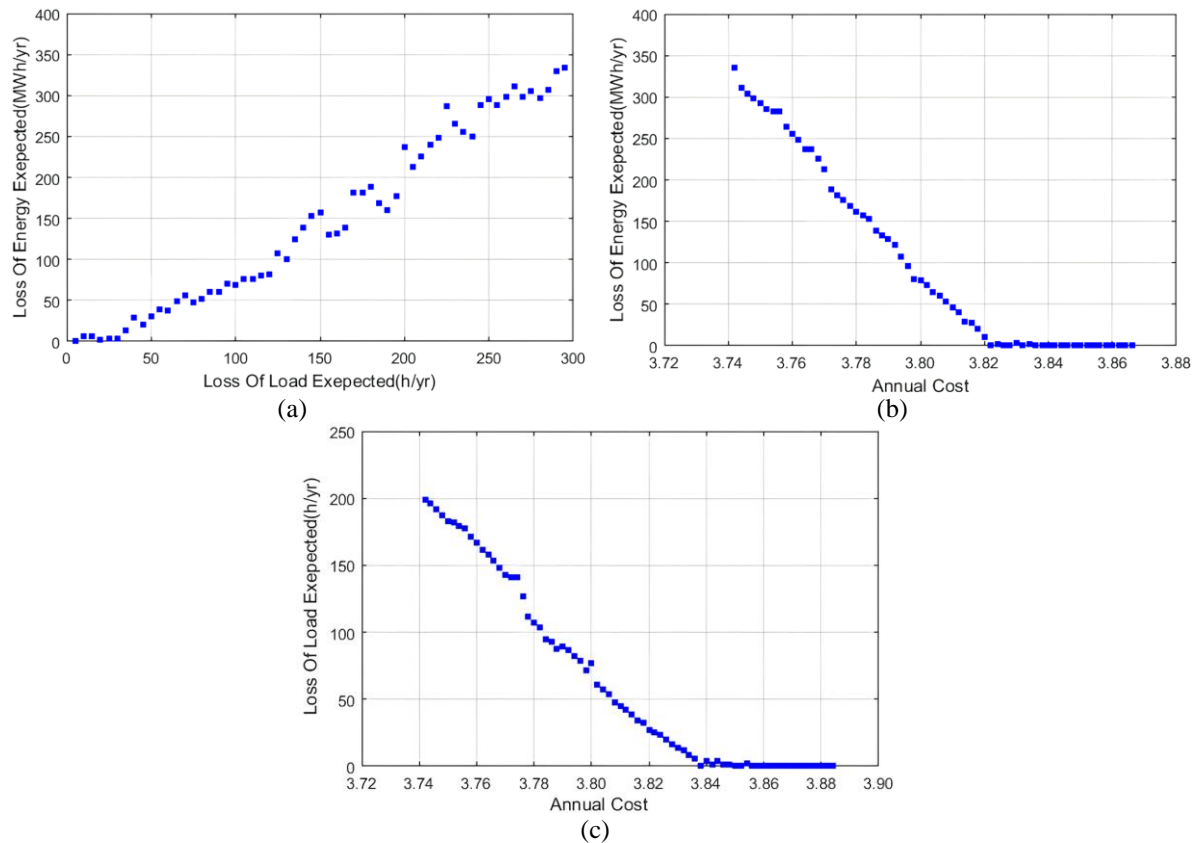

Figure 11. Cost analysis of proposed method: (a) LOEE with LOLE, (b) LOEE with annual cost, and (c) LOLE with annual cost

Table 4. Statistical analysis of proposed and conventional techniques

Methods	Mean	Median	SD
GA	1.5874	1.4791	0.5773
PSO	1.4755	1.3763	0.1491
CA	1.0675	0.9583	0.2988
CFA	1.0656	0.9462	0.2465
TSA	0.9641	0.9794	0.1146
MA-RBFNN	0.9456	0.9441	0.1068
GEO-SN^{2}L	0.9241	0.9141	0.1012
Proposed	0.9145	0.9052	0.0985

Table 5 provides a detailed comparison of the performance of the proposed and current methodologies throughout 150 trials. The conventional GA and PSO techniques have 71% and 75% accuracy rate, 66% and 68% precision, 81% and 83% recall, and 63% and 69% specificity, respectively. The CA technique has a 78% accuracy rate, 71% precision, 87% recall, and 71% specificity. The CFA technique yields results of 58% accuracy, 58% precision, 65% recall, and 56% specificity. TSA technique achieves 87% accuracy, 99% precision, 92% recall, and 90% specificity. MA-RBFNN has a precision of 99.89%, accuracy of 99.82%, recall of 99.45%, and specificity of 99.476%. The GEO-SN^{2}L algorithm has a precision of 99.90%, accuracy of 99.84%, recall of 99.59%, and specificity of 99.79%. The suggested strategy can achieve 99.91 percent accuracy, 99.85 percent precision, 99.65 percent recall, and 99.32 percent specificity. The suggested system exhibits superior accuracy, precision, recall, and specificity compared to state-of-the-art methods.

Table 5. Analysis of proposed & existing techniques for 150 No. of trials

Methods	Accuracy	Precision	Recall	Specificity
GA	71	66	81	63
PSO	75	68	83	69
CA	78	71	87	71
CFA	78	58	65	56
TSA	87	99	92	90
MA-RBFNN	99.89	99.82	99.45	99.47
GEO-SN^{2}L	99.90	99.84	99.59	99.79
Proposed	99.91	99.85	99.65	99.325

6. CONCLUSION

With a specific emphasis on renewable energy sources, this research presents the use of SBL and MAT approaches to optimize power system costs and reliability. Reducing production and operating costs while increasing power system reliability via the use of renewable energy sources is the main objective of the proposed strategy. The suggested approach is implemented on the MATLAB/Simulink platform, and its efficacy is validated. The evaluation of the suggested methodology is similar to that of the preceding methods. In addition, implementing the suggested methodology has resulted in a reduction of over 50% in the overall expenses associated with the power system. The proposed method is tested in a variety of settings, and its efficacy is evaluated using metrics like accuracy, recall, precision, and specificity, and compared to those of well-established methods like CA, CFA, TSA, MA-RBFNN, and GEO-SN2L algorithms. Results show that the suggested power system with the SBL-MAT algorithm achieves: i) 99.91% accuracy, 99.85% precision, 99.65% recall, and 99.325% specificity; and ii) Reduction in power loss and improved cost optimization and reliability.

As a prospective avenue for further investigation, it is recommended that the proposed methodology be applied to other algorithms such as HGDGEO, GJO, and GSSO. Due to the formulation and resolution of multi-objective optimization issues, the focus was only on two objectives: system dependability and cost. The challenge may be expanded to include higher goals, such as those related to system dependability, cost, volume, and weight. It is possible to use identical approaches for addressing the multi-objective issue in several domains, such as production, scheduling, marketing, assignment, transportation, and inventory. The spatial and temporal uncertainties are yet to be addressed, which shall be used to enhance the precision of modeling of the system, in both real-time and precise models. The exploration of the sharing of energy within this interconnected multivariate context remains a significant area of focus for future study.

AUTHOR CONTRIBUTIONS STATEMENT

This journal uses the Contributor Roles Taxonomy (CRediT) to recognize individual author contributions, reduce authorship disputes, and facilitate collaboration.

Name of Author	C	M	So	Va	Fo	I	R	D	O	E	Vi	Su	P	Fu
Arun Kumar Udayakumar	✓	✓	✓	✓	✓	✓		✓	✓					
P. Ashok	✓		✓		✓			✓		✓				✓
Mohan Das Raman	✓									✓				
Krishnakumar Ramasamy	✓	✓	✓	✓	✓	✓	✓		✓				✓	
Mohammad Amir	✓						✓	✓		✓	✓			

C : **C**onceptualization	I : **I**nvestigation	Vi : **Vi**sualization
M : **M**ethodology	R : **R**esources	Su : **Su**pervision
So : **So**ftware	D : **D**ata Curation	P : **P**roject administration
Va : **Va**lidation	O : Writing - **O**riginal Draft	Fu : **Fu**nding acquisition
Fo : **Fo**rmal analysis	E : Writing - Review & **E**diting	

CONFLICT OF INTEREST STATEMENT
Authors state no conflict of interest.

DATA AVAILABILITY
Data availability is not applicable to this paper as no new data were created or analyzed in this study.

REFERENCES

[1]   R. Madhana and G. Mani, "Power enhancement methods of renewable energy resources using multiport DC-DC converter: A technical review," *Sustainable Computing: Informatics and Systems*, vol. 35, 2022, doi: 10.1016/j.suscom.2022.100689.
[2]   N. Eghtedarpour and E. Farjah, "Power control and management in a Hybrid AC/DC microgrid," *IEEE Transactions on Smart Grid*, vol. 5, no. 3, pp. 1494–1505, 2014, doi: 10.1109/TSG.2013.2294275.
[3]   Z. Baig, S. B. Shivakumar, and T. Ananthapadmanabha, "A multi-objective hybrid algorithm for planning electrical distribution system," *International Journal of Electrical Engineering and Technology*, vol. 11, no. 3, pp. 66–82, 2020, doi: 10.18280/ejee.224-509.
[4]   H. Ababsia, D. Dib, and A. Djeddi, "Optimal control of the UPFC for the stability of electrical networks," *International Journal of Applied Power Engineering*, vol. 14, no. 1, pp. 180–187, 2025, doi: 10.11591/ijape.v14.i1.pp180-187.
[5]   F. Nejabatkhah and Y. W. Li, "Overview of power management strategies of hybrid AC/DC microgrid," *IEEE Transactions on Power Electronics*, vol. 30, no. 12, pp. 7072–7089, 2015, doi: 10.1109/TPEL.2014.2384999.
[6]   S. Rangasamy, S. A. Prakash, N. N. Sakhare, and U. A. Kumar, "Multiple microgrids with electric vehicle charging in a hybrid GJO-PCGAN approach for energy management," *Electrical Engineering*, 2025, doi: 10.1007/s00202-024-02922-7.
[7]   H. Mahmood, D. Michaelson, and J. Jiang, "Decentralized power management of a PV/battery hybrid unit in a droop-controlled islanded microgrid," *IEEE Transactions on Power Electronics*, vol. 30, no. 12, pp. 7215–7229, 2015, doi: 10.1109/TPEL.2015.2394351.
[8]   S. V. Kasi, N. Das, S. Alahakoon, and N. Hassan, "Effective sizing and optimization of hybrid renewable energy sources for micro distributed generation system," *IET Renewable Power Generation*, vol. 19, no. 1, p. e13193, 2025, doi: 10.1049/rpg2.13193.
[9]   K. Shafiei, A. Seifi, and M. T. Hagh, "A novel multi-objective optimization approach for resilience enhancement considering integrated energy systems with renewable energy, energy storage, energy sharing, and demand-side management," *Journal of Energy Storage*, vol. 115, p. 115966, Apr. 2025, doi: 10.1016/j.est.2025.115966.
[10] M. J. Ahmadi, "Dynamic power management and control of PV-Wind-BES based microgrid system," Nazarbayev University, 2023. [Online]. Available: https://nur.nu.edu.kz/items/7f28475f-e193-4730-8b12-6801c8ab71fe
[11] V. Narayanan, S. Kewat, and B. Singh, "Control and implementation of a multifunctional solar PV-BES-DEGS based microgrid," *IEEE Transactions on Industrial Electronics*, vol. 68, no. 9, pp. 8241–8252, 2021, doi: 10.1109/TIE.2020.3013740.
[12] N. E. Benton and M. Neil, "A critique of software defect prediction models," *IEEE Transactions on Software Engineering*, vol. 25, no. 5, pp. 675–689, 1999, doi: 10.1109/32.815326.
[13] M. Al-Saadi, M. Al-Greer, and M. Short, "Reinforcement learning-based intelligent control strategies for optimal power management in advanced power distribution systems: a survey," *Energies*, vol. 16, no. 4, p. 1608, 2023, doi: 10.3390/en16041608.
[14] K. Kanchana, T. Murali Krishna, T. Yuvaraj, and T. Sudhakar Babu, "Enhancing smart microgrid resilience under natural disaster conditions: Virtual power plant allocation using the jellyfish search algorithm," *Sustainability (Switzerland)*, vol. 17, no. 3, 2025, doi: 10.3390/su17031043.
[15] F. Wang, J. Xu, and G. Li, "A cascaded multi-port converter with energy storage units for large-scale photovoltaic systems," *CSEE Journal of Power and Energy Systems*, pp. 1–11, 2025, doi: 10.17775/CSEEJPES.2023.02270.
[16] M. Bhoopathi, V. P. Papana, C. V. K. Reddy, and U. Arun Kumar, "PV fed grid system with PI controller for enhancing power quality using CMBO-PCSANN approach," *IETE Journal of Research*, pp. 1–15, 2025, doi: 10.1080/03772063.2025.2469639.

[17] S. M. Sulthan, S. S. A., S. R. B., M. M. O., R. Veena, and I. I. A. T.P., "Centralized power management and control of a Low Voltage DC Nanogrid," *Energy Reports*, vol. 9, no. 10, pp. 1513–1520, 2023, doi: 10.1016/j.egyr.2023.07.003.

[18] J. Heidary, M. Gheisarnejad, and M. H. Khooban, "Stability enhancement and energy management of AC-DC microgrid based on active disturbance rejection control," *Electric Power Systems Research*, vol. 217, 2023, doi: 10.1016/j.epsr.2022.109105.

[19] L. Wang *et al.*, "Blockchain-based dynamic energy management mode for distributed energy system with high penetration of renewable energy," *International Journal of Electrical Power and Energy Systems*, vol. 148, 2023, doi: 10.1016/j.ijepes.2022.108933.

[20] A. T. Tran, N. T. Pham, V. Van Huynh, and D. N. M. Dang, "Stabilizing and enhancing frequency control of power system using decentralized observer-based sliding mode control," *Journal of Control, Automation and Electrical Systems*, vol. 34, pp. 541–553, 2023, doi: 10.1007/s40313-022-00979-y.

[21] R. Gugulothu, B. Nagu, and D. Pullaguram, "Energy management strategy for standalone DC microgrid system with photovoltaic/fuel cell/battery storage," *Journal of Energy Storage*, vol. 57, 2023, doi: 10.1016/j.est.2022.106274.

[22] C. S. Subash Kumar, U. Arun Kumar, K. U. Devi, and S. Ramesh, "Electricity and hydrogen fuel generation based on wind, solar energies and alkaline fuel cell: A hybrid IWGAN–AVOA approach," *Energy and Environment*, 2024, doi: 10.1177/0958305X241270218.

[23] M. Golla, K. Chandrasekaran, and S. P. Simon, "PV integrated universal active power filter for power quality enhancement and effective power management," *Energy for Sustainable Development*, vol. 61, pp. 104–117, 2021, doi: 10.1016/j.esd.2021.01.005.

[24] X. Xia and L. Xiao, "Probabilistic power flow method for hybrid AC/DC grids considering correlation among uncertainty variables," *Energies*, vol. 16, no. 6, p. 2547, 2023, doi: 10.3390/en16062547.

[25] O. Maciel C., E. Cuevas, M. A. Navarro, D. Zaldívar, and S. Hinojosa, "Side-blotched lizard algorithm: a polymorphic population approach," *Applied Soft Computing Journal*, vol. 88, 2020, doi: 10.1016/j.asoc.2019.106039.

[26] K. Ramasamy and C. S. Ravichandran, "Optimal design of renewable sources of PV/wind/FC generation for power system reliability and cost using MA-RBFNN approach," *International Journal of Energy Research*, vol. 45, no. 7, pp. 10946–10962, 2021, doi: 10.1002/er.6578.

[27] R. Krishnakumar and C. S. Ravichandran, "Reliability and cost minimization of renewable power system with tunicate swarm optimization approach based on the design of PV/Wind/FC system," *Renewable Energy Focus*, vol. 42, pp. 266–276, Sep. 2022, doi: 10.1016/j.ref.2022.07.003.

[28] Z. Wang, J. Xin, and Z. Zhang, "A novel stochastic interacting particle-field algorithm for 3D parabolic-parabolic Keller-Segel chemotaxis system," *Journal of Scientific Computing*, vol. 102, 2025, doi: 10.1007/s10915-025-02816-1.

[29] R. Sumalatha, B. V. RamiReddy, C. V. Narasimhulu, and K. Keerthi, "Voltage profile improvement in power system using an interline power flow controller and cuttlefish algorithm," *AIP Conference Proceedings*, vol. 3237, no. 1, 2025, doi: 10.1063/5.0248170.

[30] D. Li, P. Xu, X. Li, Y. Zhao, and S. Lin, "Fault detection of DFIG using an improved fractional-order PID sliding mode observer based on the adaptive golden eagle optimizer," *Journal of Electrical Engineering and Technology*, vol. 20, pp. 501–515, 2024, doi: 10.1007/s42835-024-01965-x.

BIOGRAPHIES OF AUTHORS

Dr. Arun Kumar Udayakumar 🆔 📊 SC ◐ received his Ph.D. in the field of Electrical Engineering, and his area of research includes power quality improvement, brushless DC motor drives, artificial intelligence, internet of things and optical sensors and electronics, and solar absorbers. He currently works as a professor and researcher at Karpagam Academy of Higher Education (Deemed to be University), Coimbatore, India. He has published more than 50 papers in well-reputed journals and conferences, including IEEE, Springer, Elsevier, and American Scientific Publishers. He has also received funds from Texas Instruments, Bengaluru, India, towards his research project entitled "Implementation of Sliding Mode based Position Sensorless Drive for PMSM", qualifying for the quarter final in "Texas Instruments Innovation Challenge, India Design Contest 2015". He has also received $300 worth of components from DST - Texas Instruments, towards his research work in PMSM. As a reviewer, he has reviewed more than 100 articles from various journals, including IEEE, Springer, and Elsevier. He has also served as an editorial board member and advisory committee member for various IEEE international and national conferences. He can be contacted at email: arun.udayakumarn@gmail.com.

Dr. P. Ashok 🆔 📊 SC ◐ is from Chennai, Tamil Nadu, India. He is currently employed as an Associate Professor at Symbiosis Institute of Digital and Telecom Management (SIDTM), affiliated to Symbiosis International (Deemed University), Pune. His areas of interest include Optical Communication, Wireless Communication, Transmission Lines and Waveguides, Antennas, and Wave Propagation. He does active research in the field of Quantum Cascade Lasers, where he has published high-quality papers in reputed journals along with his research supervisor, Dr. M. Ganesh Madhan. He is an active participant in International and National Conferences organized by reputed institutions in India. His passion for teaching and learning is evident in his career. His ability to make complex things simple is his way of teaching. He also has 3 patents to his credit in the field of IoT. He has close to 52 high-quality research articles indexed in Scopus. He can be contacted at email: p.ashok@sidtm.edu.in.

Mohan Das Raman 🆔 📇 SC ⊙ received a B.E. in EEE from CSI Engineering College in 2002 and a master's degree in Power Electronics and Drives from Karunya University in 2007, and a Ph.D. in Electrical Engineering from Anna University, Chennai in 2020. He is currently working as an associate professor in the Department of Electrical and Electronics Engineering at New Horizon College of Engineering, Bengaluru, Karnataka, India. His research interests include power converters, harmonic mitigation, electric vehicles, and soft computing techniques. He can be contacted at email: mohandas@newhorizonindia.edu.

Krishnakumar Ramasamy 🆔 📇 SC ⊙ received B.E. degree in Electrical and Electronics Engineering from K.S.Rangasamy College of Technology, Tiruchengode, affiliated to Anna University, Chennai, in 2009. M.E degree in Industrial Engineering from Kumaraguru College of Technology, Coimbatore, affiliated to Anna University, Chennai, in 2011. He received a Doctor of Philosophy in the area of power system reliability from Anna University, Chennai, in the year 2021. His research interests include power system reliability, renewable energy systems, and electric vehicles. He can be contacted at email: krishnakumar.ramasamy@srec.ac.in.

Mohammad Amir 🆔 📇 SC ⊙ received the B.Tech. degree in electrical engineering from Integral University, Lucknow, India, in 2015, the M.Tech. degree from the Department of Electrical Engineering, Madan Mohan Malaviya University of Technology (MMMUT), Gorakhpur, India, in 2018, and the Ph.D. degree (Hons.) from the Department of Electrical Engineering, Jamia Millia Islamia University, Delhi, New Delhi, India, in 2023. He is currently a Senior Researcher with the Department of Electrical Engineering, Indian Institute of Technology Delhi (IIT), India. Additionally, he is leading a research project as the Principal Investigator (PI) funded by the Science and Engineering Research Board with a grant of 3.03 million INR. He engaged as a Visiting Research Associate with the Department of Electrical Engineering, Qatar University, and contributed to the National Priorities Research Program Project. He was a Research Assistant with the Advanced Power Electronics Research Laboratory, Department of Electrical Engineering, JMI, from January 2021 to February 2023, working under the SPARC Project of MHRD, Government of India, in collaboration with Aalborg University, Denmark. His research interests include renewable energy, intelligent energy management, energy storage, electric vehicles, power system optimization, and smart microgrids. He can be contacted at email: md.amir@ieee.org.